

Studying Steady Shear Flow Characteristics of Entangled Polymer Solutions with Parallel Mechanical Superposition

Xin Li and Shi-Qing Wang*

Department of Polymer Science, University of Akron, Akron, Ohio 44325-3909

Received April 20, 2010; Revised Manuscript Received May 22, 2010

ABSTRACT: We probe the nature of steady shear flow of entangled polymer solutions by superimposing either small amplitude oscillatory shear or small step strain and analyzing the resultant mechanic responses. Our results show that (a) polymer dynamics (in terms of stress relaxation) are accelerated relative to the quiescent dynamics in direct proportion to the underlying shear rate and (b) the steady shear is a viscous state where chains are displaced past one another on a time scale of the reciprocal rate, consistent with the idea of convective constraint release.

I. Introduction

Deformation and flow behavior of entangled polymeric liquids is a central subject in polymer science and has been extensively studied in the past^{1,2} using conventional rheometric methods. To link macroscopic rheological measurements to molecular responses, numerous calculations based on different versions of the tube model³ have been successfully carried out.^{4,5} Such theoretical studies have also been extended to the nonlinear response regime.^{6,7}

A recent series of particle-tracking velocimetric (PTV) observations along with rheometric measurements have increased our understanding of mechanical responses of entangled polymers to startup continuous shear.⁸ For well-entangled polymer solutions and melts, appearance of shear inhomogeneity during sudden startup shear has provided convincing evidence for yielding⁹ that takes place on time scales much shorter than the reptation time and precedes the eventual state of steady shear. These new findings indicate that we need to think about how the transient cohesion of the entanglement network is overcome during fast continuous shear⁸ or after a sudden step shear.¹⁰ In particular, the emergence of shear banding seems to originate from localized cohesive failure (i.e., yielding) during the initial response to sudden fast shear. The observed shear banding is so long-lived for well-entangled polymers that it remains elusive whether homogeneous shear would ever be recovered as external shearing continues indefinitely.

There have been two recent studies of the nature of steady shear in the shear thinning regime of entangled solutions. To a series of polybutadiene solutions,¹¹ startup shear was first applied to produce steady state. Then, the shear was turned off for different amounts of resting time τ_{Rest} before the same startup shear was reapplied. The stress overshoot characteristics were found to return only after sufficient resting time τ_{Rest} from the preceding shear, which was found to be longer than the terminal relaxation time τ . The weaker overshoot was taken as evidence for chain disentanglement.¹¹ In a second study, by superimposing small amplitude oscillatory shear at different frequencies onto a steady-state shear in the shear thinning regime, it was found based on entangled solutions¹² that the state of steady flow possesses a basic characteristic: the effective relaxation time is

universally shorter than the reciprocal imposed average shear rate $\dot{\gamma}$ regardless of whether steady shear is homogeneous or not. When the Weissenberg number $Wi = \dot{\gamma}\tau$ is much greater than unity, chains bypass one another by undergoing convective constraint release (CCR)¹³ on the time scale of $1/\dot{\gamma} \ll \tau$. Such state of flow is truly a state of less entanglement or partial disentanglement because in quiescence with full entanglement chains take a period comparable to τ to pass around one another by thermal diffusion.

PTV observations have offered us fresh insight into such prominent features as stress overshoot during startup shear. Yielding, i.e., a transition from elastic deformation to irrecoverable deformation (i.e., flow) that is signified by the stress overshoot,¹⁴ can also occur in absence of any visible shear inhomogeneity, as is the case whenever the system is insufficiently entangled.^{8b,d} Shear homogeneity allows us to more straightforwardly explore various rheological characteristics of steady shear of entangled polymers.

In the present study, we further explore the nature of homogeneous steady-state shear of entangled solutions beyond the yield point, i.e., beyond the shear stress overshoot, by examining additional rheological responses in the steady state to superimposed small external mechanical perturbations.

II. Experimental Section

A. Materials. In order to achieve steady state without edge fracture, entangled solutions were prepared involving a low concentration of 3% and ultrahigh molecular weight 1,4-polybutadiene with $M_w = 2600$ kg/mol and $M_n = 1600$ kg/mol from Bridgestone-America. Two oligomeric polybutadienes were used as solvent to make two 3% solutions: one being monodisperse with $M_w = 9$ kg/mol from Bridgestone-America and the other from Aldrich with $M_w = 1.8$ kg/mol and a high level of vinyl content (category number 20,043-3). In this report, the PB solutions in solvent PB9K and PB1.8K are respectively labeled as PB2.6M-3%-9K and PB2.6M-3%-1.8K.

The glass transition temperatures T_g of the pure PB melt of 2.6M and 9K are around -98 °C. In contrast, T_g of PB1.8K is ca. -38 °C. The sample was prepared by first dissolving the high molecular weight polybutadiene in toluene and then mixing with oligomer. Toluene was then allowed to evaporate from the uniform solution at room temperature for a week under the hood. The residual toluene was removed under vacuum for about 3 days.

*Corresponding author. E-mail: swang@uakron.edu.

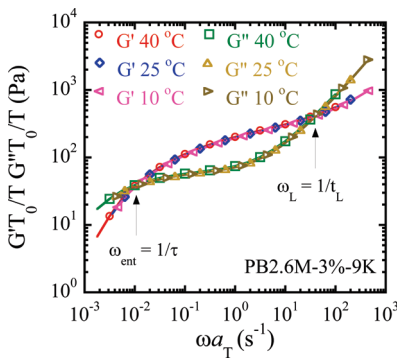


Figure 1. Storage and loss moduli G' and G'' of PB2.6M-3%-9K at a reference temperature of 40 °C where the curves at 10 and 25 °C were shifted horizontally by a shift factor of $a_{10^\circ\text{C}} = 4.6$ and $a_{25^\circ\text{C}} = 2.1$, respectively.

Table 1

temp (°C)	PB2.6M-3%-9K		PB2.6M-3%-1.8K	
	ω_c (s ⁻¹)	ω_L (s ⁻¹)	ω_c (s ⁻¹)	ω_L (s ⁻¹)
10	2.4×10^{-3}	8.9	2.8×10^{-4}	0.35
25	5.3×10^{-3}	20.0	1.3×10^{-3}	2.9
40	1.1×10^{-2}	38.6	3.6×10^{-3}	14.5

B. Methods. All the rheological measurements were carried out using a controlled-torque rheometer (Physica MCR-301, Anton Paar) in a cone–plate cell of 25 mm diameter with a 2° cone angle. In controlled stress (CS) mode, this rheometer has the ability to perform oscillatory shear superimposed onto a steady simple shear. In such a parallel superposition SAOS experiment, we first apply a constant shear rate in the control rate (CR) mode until steady state. Then, the rheometer was programmed to switch to the CS mode to match the steady-state shear stress; meanwhile, a SAOS was superimposed. Our second experimental protocol consists of a short “pulse” in the applied rate during steady-state shear when the shear rate is elevated for a very short duration, which amounts to performing a step strain and stress relaxation against a steady shear baseline.

III. Results and Discussion

A. Linear Viscoelastic Characters and Temperature Dependence. Small amplitude oscillatory shear (SAOS) measurements were first performed to characterize linear viscoelastic properties of these two solutions at several temperatures. Figure 1 shows the dynamic modulus curves for PB2.6M-3%-9K, measured at three temperatures. The collapse indicates existence of time–temperature superposition within the explored frequency range.

Table 1 lists the crossover frequency ω_c on the lower branch and ω_L at high frequencies at temperatures of 10, 25, and 40 °C. From Table 1, we get the WLF Shifting factor of PB2.6M-3%-9K at a reference temperature of 40 °C $a_T = \tau(T)/\tau(T_0) = \omega_c(T_0)/\omega_c(T)$ equal to 2.1 for $T = 25$ °C and 4.6 for $T = 10$ °C. The ω_c of PB2.6M-3%-1.8K at 10 °C is estimated from the trend of its G' and G'' curves.

To examine the validity of the time–temperature superposition principle in continuous shear, we apply startup shear to PB2.6M-3%-9K at three rates at three temperatures such that the effective rate, i.e., the normalized shear rate Weissenberg number Wi , is the same. Figure 2 shows the stress vs strain at temperatures of 10, 25, and 40 °C at $Wi = 11$. The perfect overlapping indicates that the dominant rheological responses obey the WLF relationship. We have also studied the temperature dependence by performing small step strain tests to determine how the stress relaxation dynamics vary with temperature. Figure 3 shows that the stress relaxation behavior

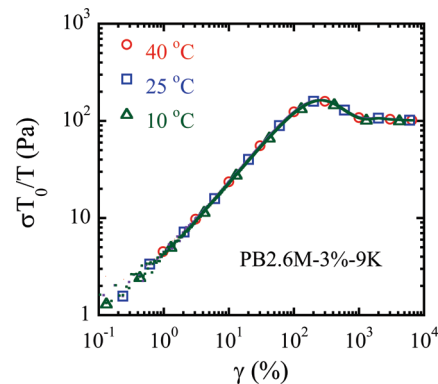


Figure 2. Stress vs strain upon startup shear at $Wi = 11$ at respective temperatures of 10, 25, and 40 °C. In this and all the following figures, instead of using all the available data points to make the plots that form nearly continuous curves and overlap among the different data sets, we select a few point from each set to avoid overlapping.

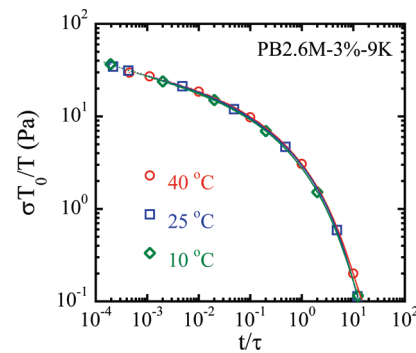


Figure 3. Stress relaxation from a small step strain of 10% produced with a shear rate of 1 s⁻¹.

can be depicted at different temperatures by rescaling the time with the terminal relaxation time.

B. Superimposed SAOS at Different Temperatures. Despite extensive efforts to describe rheological behavior of entangled polymeric liquids, the state of steady shear flow has essentially escaped a first-principles treatment. For example, the tube model can only depict steady shear properties such as shear thinning by introducing the effect of convective constraint release (CCR).¹³ The idea behind CCR is to recognize that the dominant molecular relaxation time in presence of shear is accelerated in proportion to the reciprocal shear rate. In other words, the effective chain relaxation dynamics in shear is no longer Brownian diffusion in origin.

One way to measure indirectly the effective relaxation time τ_{eff} in steady shear is to superimpose small amplitude oscillatory shear (SAOS) during steady shear, which is a well-established technique.^{1,15–18} In this method, SAOS frequency sweep measurement is carried out to evaluate G' and G'' curves against the baseline. We would like to apply the method of the parallel superimposed SAOS to examine any temperature dependence of τ_{eff} at the same applied shear rate. A lack of any temperature dependence would confirm that the accelerated chain bypassing each other is not dictated by thermal diffusion. Figure 4 shows that the structure of the G' and G'' curves in the “terminal regime” remains unchanged although the Brownian dynamics have slowed down by a factor of 4.6 from 40 to 10 °C. In other words, despite the temperature change, the three curves cross at essentially the same frequency around 0.2 rad/s = $1/\tau_{\text{eff}}$, which is about 5 times higher than the applied rate $\dot{\gamma} = 0.04$ s⁻¹. We have carried out similar tests at other applied rates at these temperatures for this and the other solution. All the data conform to one

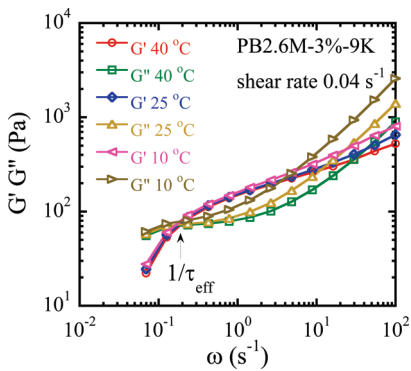


Figure 4. Extracted G' and G'' curves vs ω in steady shear at a rate of 0.04 s^{-1} at temperatures 10, 25, and 40°C , where the crossover frequency, $1/\tau_{\text{eff}}$, indicates the accelerated chain dynamics by the applied shear.

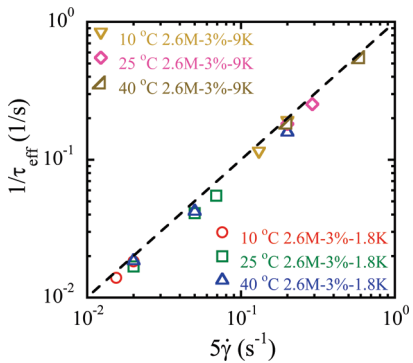


Figure 5. Characteristic relaxation rate $1/\tau_{\text{eff}}$ in the presence of steady shear at the different applied rates and three temperatures in two different solutions is plotted against $5\dot{\gamma}$, showing a universal correlation, independent of temperature.

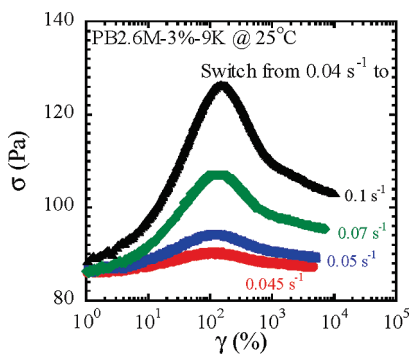


Figure 6. Stress change as a function of elapsed strain upon switching from steady state at $\dot{\gamma} = 0.04 \text{ s}^{-1}$ to $0.045, 0.05, 0.07$, and 0.1 s^{-1} .

universal scaling law as shown in Figure 5, which is in complete numerical agreement with a previous report.¹²

C. Stepwise Rate Jump in Shear Thinning Regime. We have carried out a sequence of stepwise rate jump and monitored the stress growth over time. Figure 6 shows stress response in a series of discrete rate switching experiments from the steady state at a rate of 0.04 s^{-1} . According to Figure 5, the effective relaxation rate $1/\tau_{\text{eff}}$ should be ca. $5\dot{\gamma} \sim 0.2 \text{ s}^{-1}$. If we take this effective relaxation time literally, then any rate jump with a magnitude lower than 0.2 s^{-1} would only result in a monotonic change in the measured stress. Instead, stress overshoot emerges in each of these rate switching experiments that involves a rate increment as low as 0.005 s^{-1} . This experiment appears to suggest that the steady state shear is a state of complete balance between intrachain retraction force

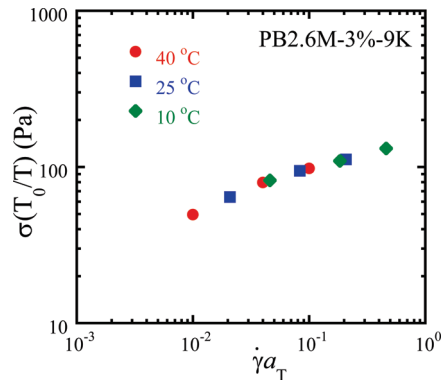


Figure 7. Master flow curves made of steady shear stress vs rate data at three temperatures of 40, 25, and 10°C where the reference temperature is 40°C and the WLF shifting factor is the same as that in Figure 1.

and interchain gripping force.⁹ An increase in the applied rate automatically results in high interchain gripping force that produces additional chain deformation. The additional chain deformation ceases when a point of force imbalance is reached at the stress peak, i.e., the point of stress overshoot as shown in Figure 6. The outcome of this experiment indicates that the meaning of τ_{eff} is not entirely equivalent to the quiescent terminal relaxation time τ .

D. Master Flow Curve in Steady Shear. At a given temperature in the shear thinning regime, the shear stress increases little with increasing applied rate as shown in Figure 7 because the chains are more oriented at a higher rate and thus offer less viscous resistance among each other during shear. Changing temperature has the consequence of changing the Brownian dynamics as well as viscous interactions among chains. The collapse of three sets of data at three temperatures onto a master flow curve in Figure 7 shows that the WLF shifting factor $a_T = \tau(T)/\tau(T_0) = T_0\eta(T,\dot{\gamma})/T\eta(T_0,\dot{\gamma}a_T)$. In other words, the steady shear-thinning “viscosity” η/T scales with temperature in the same manner as the quiescent terminal relaxation time τ as long as the viscosity $\eta(T,\dot{\gamma})$ is evaluated at the same effective shear rate, i.e., the same Weissenberg number $Wi = \dot{\gamma}\tau$.

E. Step Strain Relaxation during Steady Shear. The effective relaxation rate evaluated from parallel superposition of SAOS in steady shear, e.g., from Figure 4, is found to be proportional to the applied rate as shown in Figure 5. Indeed, the state of steady shear must correspond to chains passing around one another on the time scale of the reciprocal shear rate. To further probe the nature of the steady state in the shear thinning regime, we introduce a more direct means to probe the effect of steady shear on the chain dynamics, i.e., superimposing a step strain during steady shear. Previously, such a superposition has been used to measure the elastic modulus of polystyrene solutions in steady shear.¹⁹

For reference, we first performed a stress relaxation experiment for a small step strain of 10% in PB2.6M-3%-9K at 25°C . Then, we produced a steady shear at a shear rate of 0.0003 s^{-1} ($Wi < 0.1$) in the terminal (Newtonian) regime. A small step strain of 10% is superimposed onto this steady shear. The resulting elevation of the shear stress level relaxed over time toward the steady state value. Figure 8 shows that the stress relaxation in presence of this Newtonian flow is identical to that observed in a standard stress relaxation test. On the other hand, if the same superposition of a small step strain was performed over a steady shear in the shear thinning regime, i.e., at a shear rate $\dot{\gamma} = 0.04 \text{ s}^{-1}$, we can also evaluate the dynamics associated with the stress relaxation by subtraction from the baseline, i.e., the steady shear stress

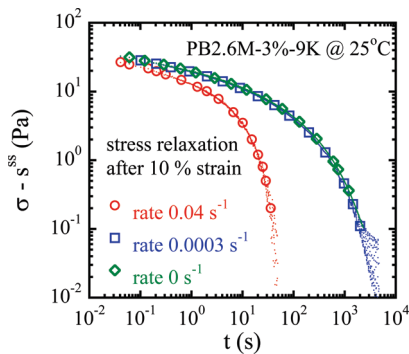


Figure 8. Parallel superposition of step strain (the superimpose step strain is 10%, produced with a shear rate of 1 s^{-1}) for PB2.6M-3%-9K at 25°C under the shear rate of 0.04 s^{-1} , 0.0003 s^{-1} , and in absence of shear. The data were obtained by subtracting from the baseline, i.e., steady state shear stress.

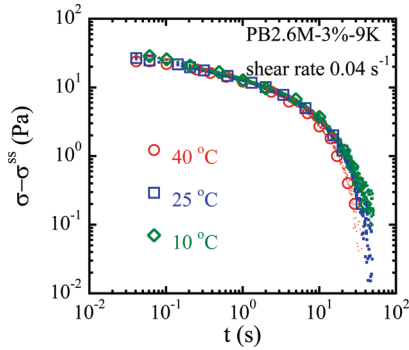


Figure 9. Parallel superposition step strain (the superimpose step strain is 10% produced with a shear rate of 1 s^{-1}) for PB2.6M-3%-9K at different temperatures under the same shear rate of 0.04 s^{-1} . The data were obtained by subtracting from the baseline, i.e., steady state shear stress.

value. In contrast to the relaxation dynamics in quiescence or in Newtonian regime, the dynamics are much faster. Moreover, the same dynamics are observed at three different temperatures as shown in Figure 9, consistent with the data in Figure 4. It affirms that the stress relaxation is not dictated by Brownian motions and is determined by the underlying shear that pulls the chains out of the deformed entanglement network to accelerate the stress relaxation.

Lastly, we superimpose the same small (10%) step strain against steady shear at different rates for the other solution of PB2.6M-3%-1.8K. Figure 10a shows the stress relaxation dynamics to be controlled by the underlying shear rate. The faster relaxation is apparently realized by the higher rate of underlying shear. Instead of relaxing via Brownian motions indicated by the slowest relaxation data (0 s^{-1}) in Figure 10a, the strained network more quickly “dissolves” due to the convective effect of the underlying shear. Actually three relaxation curves in Figure 10a collapse onto one upon normalizing the time with the underlying shear rate as shown in Figure 10b. The small perturbation in the stress due to the step strain of 10% quickly vanishes on the time scale of $1/\dot{\gamma}$. Therefore, these superimposed step strain tests further clarify the nature of steady shear in entangled polymers: stress relaxation and chain dynamics are accelerated from those observed in the quiescence to time scales comparable to the reciprocal shear rate. In other words, the state of steady flow is one where chains are displaced to pass by one another by the external condition (the moving surface). In contrast, in terminal steady flow, chains “voluntarily” pass by one another by thermal diffusion (i.e., Brownian motion).

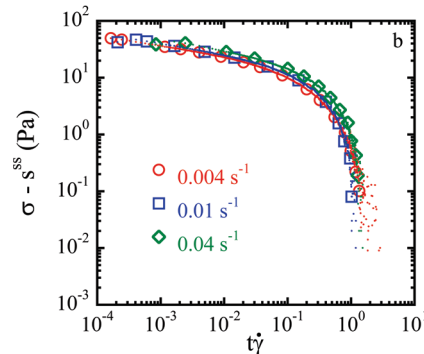
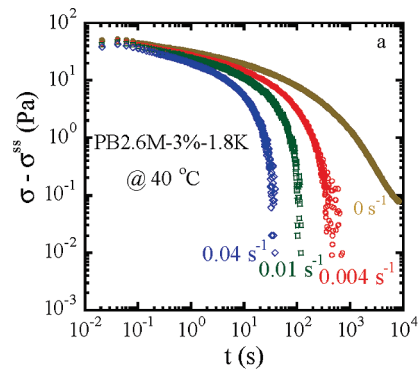


Figure 10. (a) Stress relaxation curve for PB2.6M-3%-1.8K at equilibrium and under different steady shear rates at 40°C . The data were obtained by subtracting from the baseline, i.e., steady state shear stress. (b) Master curves obtained by scaling the time scale with the underlying shear rate.

IV. Summary

The nature of steady shear flow of entangled polymeric liquids has been somewhat elusive even without such complications as shear inhomogeneity and edge fracture. In quiescence, chain dynamics and stress relaxation behavior are dictated by thermal diffusion processes. Often the time–temperature superposition principle, as empirically depicted by the WLF relation, can be applied to extend our observation of linear viscoelasticity. In the regime of nonlinear responses, Brownian dynamics play a less important role and cannot control polymer dynamics during steady shear as long as the imposed shear rate exceeds the quiescent chain relaxation rate. On the basis of entangled solutions that only experience homogeneous shear, we carried out both parallel superposition of small amplitude oscillatory shear and small step strain to explore the steady shear properties. Figures 4 and 9 convincingly show that the state of steady shear is one where chains are being brought past one another at a rate equal to the imposed shear rate, independent of temperature. Although Brownian motions are faster at higher temperatures, they are ineffective in dictating the dynamic responses as long as the imposed rate is faster than the quiescent terminal relaxation rate. Figure 10a,b shows that indeed the imposed rate governs the chain dynamics during steady shear and polymer dynamics can be significantly accelerated beyond those in quiescence due to the convective constraint release.

Acknowledgment. This work is supported, in part, by a grant (DMR-0821697) from the National Science Foundation.

References and Notes

- (1) Ferry, J. D. *Viscoelastic Properties of Polymers*; John Wiley & Sons: New York, 1980.
- (2) Bird, R. B.; Curtiss, C. F.; Armstrong, R. C.; Hassager, O. *Dynamics of Polymeric Liquids: Kinetic Theory*; John Wiley & Sons: New York, 1987; Vol. 2.

(3) Doi, M.; Edwards, S. F. *The Theory of Polymer Dynamics*; Cambridge University Press: New York, 1986.

(4) McLeish, T. C. B. *Adv. Phys.* **2002**, *51*, 1379.

(5) Watanabe, H. *Prog. Polym. Sci.* **1999**, *24*, 1253.

(6) Mead, D. W.; Larson, R. G.; Doi, M. *Macromolecules* **1998**, *31*, 7895.

(7) Graham, R. S.; Likhtman, A. E.; McLeish, T. C. B. *J. Rheol.* **2003**, *47*, 1171.

(8) (a) Tapadia, P.; Wang, S. Q. *Phys. Rev. Lett.* **2006**, *96*, 016001. (b) Ravindranath, S.; Wang, S. Q. *Macromolecules* **2008**, *41*, 2663. (c) Ravindranath, S.; Wang, S. Q. *J. Rheol.* **2008**, *52*, 957. (d) Boukany, P. E.; Wang, S. Q. *J. Rheol.* **2009**, *53*, 73.

(9) (a) Wang, S. Q.; Ravindranath, S.; Wang, Y.; Boukany, P. *J. Chem. Phys.* **2007**, *127*, 064903. (b) Wang, Y. Y.; Wang, S. Q. *J. Rheol.* **2009**, *53*, 1389.

(10) (a) Ravindranath, S.; Wang, S. Q. *Macromolecules* **2007**, *40*, 8031. (b) Boukany, P. E.; Wang, S. Q. *Macromolecules* **2009**, *42*, 6261.

(11) Robertson, C. G.; Warren, S.; Plazek, D. J.; Roland, C. M. *Macromolecules* **2004**, *37*, 10018.

(12) Boukany, P. E.; Wang, S. Q. *J. Rheol.* **2009**, *53*, 1425.

(13) Marrucci, G. *J. Non-Newtonian Fluid Mech.* **1996**, *62*, 279.

(14) Boukany, P. E.; Wang, S. Q. *J. Rheol.* **2009**, *53*, 617.

(15) Macdonald, I. F. *Trans. Soc. Rheol.* **1973**, *17*, 537.

(16) Isayev, A. I.; Wong, C. M. *J. Polym. Sci., Part B: Polym. Phys.* **1988**, *26*, 2303.

(17) Costello, B. A. D. *J. Non-Newtonian Fluid Mech.* **1997**, *68*, 303.

(18) Somma, E.; Valentino, O.; Titomanlio, G.; Ianniruberto, G. *J. Rheol.* **2007**, *51*, 987.

(19) Archer, L. A. *J. Rheol.* **1999**, *43*, 1617.